Open access • Journal Article • DOI:10.1103/PHYSREVLETT.111.081801

Measurement of Atmospheric Neutrino Oscillations with IceCube — Source link

M. G. Aartsen, Rasha Abbasi, Y. Abdou, Markus Ackermann ...+284 more authors

Institutions: University of Adelaide, University of Wisconsin-Madison, Ghent University, University of Canterbury ...+34 more institutions

Published on: 19 Aug 2013 - Physical Review Letters (American Physical Society)

Topics: IceCube Neutrino Observatory, Neutrino detector, Neutrino, Neutrino oscillation and Solar neutrino problem

Measurement of Atmospheric Neutrino Oscillations with IceCube

M. G. Aartsen,[2] R. Abbasi,[27] Y. Abdou,[22] M. Ackermann,[42] J. Adams,[15] J. A. Aguilar,[21] M. Ahlers,[27] D. Altmann,[9] J. Auffenberg,[27] X. Bai,[31,*] M. Baker,[27] S. W. Barwick,[23] V. Baum,[28] R. Bay,[7] J. J. Beatty,[17,18] S. Bechet,[12] J. Becker Tjus,[10] K.-H. Becker,[41] M. Bell,[39] M. L. Benabderrahmane,[42] S. BenZvi,[27] J. Berdermann,[42] P. Berghaus,[42] D. Berley,[16] E. Bernardini,[42] A. Bernhard,[30] D. Bertrand,[12] D. Z. Besson,[25] G. Binder,[8,7] D. Bindig,[41] M. Bissok,[1] E. Blaufuss,[16] J. Blumenthal,[1] D. J. Boersma,[40] S. Bohaichuk,[20] C. Bohm,[34] D. Bose,[13] S. Böser,[11] O. Botner,[40] L. Brayeur,[13] H.-P. Bretz,[42] A. M. Brown,[15] R. Bruijn,[24] J. Brunner,[42] M. Carson,[22] J. Casey,[5] M. Casier,[13] D. Chirkin,[27] A. Christov,[21] B. Christy,[16] K. Clark,[39] F. Clevermann,[19] S. Coenders,[1] S. Cohen,[24] D. F. Cowen,[39,38] A. H. Cruz Silva,[42] M. Danninger,[34] J. Daughhetee,[5] J. C. Davis,[17] C. De Clercq,[13] S. De Ridder,[22] P. Desiati,[27] M. de With,[9] T. DeYoung,[39] J. C. Díaz-Vélez,[27] M. Dunkman,[39] R. Eagan,[39] B. Eberhardt,[28] J. Eisch,[27] R. W. Ellsworth,[16] S. Euler,[1] P. A. Evenson,[31] O. Fadiran,[27] A. R. Fazely,[6] A. Fedynitch,[10] J. Feintzeig,[27] T. Feusels,[22] K. Filimonov,[7] C. Finley,[34] T. Fischer-Wasels,[41] S. Flis,[34] A. Franckowiak,[11] R. Franke,[42] K. Frantzen,[19] T. Fuchs,[19] T. K. Gaisser,[31] J. Gallagher,[26] L. Gerhardt,[8,7] L. Gladstone,[27] T. Glüsenkamp,[42] A. Goldschmidt,[8] G. Golup,[13] J. G. Gonzalez,[31] J. A. Goodman,[16] D. Góra,[42] D. T. Grandmont,[20] D. Grant,[20] A. Groß,[30,†] C. Ha,[8,7] A. Haj Ismail,[22] P. Hallen,[1] A. Hallgren,[40] F. Halzen,[27] K. Hanson,[12] D. Heereman,[12] D. Heinen,[1] K. Helbing,[41] R. Hellauer,[16] S. Hickford,[15] G. C. Hill,[2] K. D. Hoffman,[16] R. Hoffmann,[41] A. Homeier,[11] K. Hoshina,[27] W. Huelsnitz,[16,‡] P. O. Hulth,[34] K. Hultqvist,[34] S. Hussain,[31] A. Ishihara,[14] E. Jacobi,[42] J. Jacobsen,[27] K. Jagielski,[1] G. S. Japaridze,[4] K. Jero,[27] O. Jlelati,[22] B. Kaminsky,[42] A. Kappes,[9] T. Karg,[42] A. Karle,[27] J. L. Kelley,[27] J. Kiryluk,[35] F. Kislat,[42] J. Kläs,[41] S. R. Klein,[8,7] J.-H. Köhne,[19] G. Kohnen,[29] H. Kolanoski,[9] L. Köpke,[28] C. Kopper,[27] S. Kopper,[41] D. J. Koskinen,[39] M. Kowalski,[11] M. Krasberg,[27] K. Krings,[1] G. Kroll,[28] J. Kunnen,[13] N. Kurahashi,[27] T. Kuwabara,[31] M. Labare,[13] H. Landsman,[27] M. J. Larson,[37] M. Lesiak-Bzdak,[35] M. Leuermann,[1] J. Leute,[30] J. Lünemann,[28] J. Madsen,[33] R. Maruyama,[27] K. Mase,[14] H. S. Matis,[8] F. McNally,[27] K. Meagher,[16] M. Merck,[27] P. Mészáros,[38,39] T. Meures,[12] S. Miarecki,[8,7] E. Middell,[42] N. Milke,[19] J. Miller,[13] L. Mohrmann,[42] T. Montaruli,[21,§] R. Morse,[27] R. Nahnhauer,[42] U. Naumann,[41] H. Niederhausen,[35] S. C. Nowicki,[20] D. R. Nygren,[8] A. Obertacke,[41] S. Odrowski,[30] A. Olivas,[16] M. Olivo,[10] A. O'Murchadha,[12] A. Palazzo,[43] L. Paul,[1] J. A. Pepper,[37] C. Pérez de los Heros,[40] C. Pfendner,[17] D. Pieloth,[19] E. Pinat,[12] N. Pirk,[42] J. Posselt,[41] P. B. Price,[7] G. T. Przybylski,[8] L. Rädel,[1] M. Rameez,[21] K. Rawlins,[3] P. Redl,[16] R. Reimann,[1] E. Resconi,[30] W. Rhode,[19] M. Ribordy,[24] M. Richman,[16] B. Riedel,[27] J. P. Rodrigues,[27] C. Rott,[36] T. Ruhe,[19] B. Ruzybayev,[31] D. Ryckbosch,[22] S. M. Saba,[10] T. Salameh,[39] H.-G. Sander,[28] M. Santander,[27] S. Sarkar,[32] K. Schatto,[28] M. Scheel,[1] F. Scheriau,[19] T. Schmidt,[16] M. Schmitz,[19] S. Schoenen,[1] S. Schöneberg,[10] A. Schönwald,[42] A. Schukraft,[1] L. Schulte,[11] O. Schulz,[30] D. Seckel,[31] Y. Sestayo,[30] S. Seunarine,[33] C. Sheremata,[20] M. W. E. Smith,[39] D. Soldin,[41] G. M. Spiczak,[33] C. Spiering,[42] M. Stamatikos,[17,‖] T. Stanev,[31] A. Stasik,[11] T. Stezelberger,[8] R. G. Stokstad,[8] A. Stößl,[42] E. A. Strahler,[13] R. Ström,[40] G. W. Sullivan,[16] H. Taavola,[40] I. Taboada,[5] A. Tamburro,[31] A. Tepe,[41] S. Ter-Antonyan,[6] G. Tešić,[39] S. Tilav,[31] P. A. Toale,[37] S. Toscano,[27] M. Usner,[11] D. van der Drift,[8,7] N. van Eijndhoven,[13] A. Van Overloop,[22] J. van Santen,[27] M. Vehring,[1] M. Voge,[11] M. Vraeghe,[22] C. Walck,[34] T. Waldenmaier,[9] M. Wallraff,[1] R. Wasserman,[39] Ch. Weaver,[27] M. Wellons,[27] C. Wendt,[27] S. Westerhoff,[27] N. Whitehorn,[27] K. Wiebe,[28] C. H. Wiebusch,[1] D. R. Williams,[37] H. Wissing,[16] M. Wolf,[34] T. R. Wood,[20] K. Woschnagg,[7] C. Xu,[31] D. L. Xu,[37] X. W. Xu,[6] J. P. Yanez,[42] G. Yodh,[23] S. Yoshida,[14] P. Zarzhitsky,[37] J. Ziemann,[19] S. Zierke,[1] and M. Zoll[34]

(IceCube Collaboration)

[1]*III. Physikalisches Institut, RWTH Aachen University, D-52056 Aachen, Germany*
[2]*School of Chemistry and Physics, University of Adelaide, Adelaide South Australia, 5005 Australia*
[3]*Department of Physics and Astronomy, University of Alaska Anchorage, 3211 Providence Drive, Anchorage, Alaska 99508, USA*
[4]*CTSPS, Clark-Atlanta University, Atlanta, Georgia 30314, USA*
[5]*School of Physics and Center for Relativistic Astrophysics, Georgia Institute of Technology, Atlanta, Georgia 30332, USA*
[6]*Department of Physics, Southern University, Baton Rouge, Louisiana 70813, USA*
[7]*Department of Physics, University of California, Berkeley, California 94720, USA*
[8]*Lawrence Berkeley National Laboratory, Berkeley, California 94720, USA*
[9]*Institut für Physik, Humboldt-Universität zu Berlin, D-12489 Berlin, Germany*
[10]*Fakultät für Physik and Astronomie, Ruhr-Universität Bochum, D-44780 Bochum, Germany*
[11]*Physikalisches Institut, Universität Bonn, Nussallee 12, D-53115 Bonn, Germany*

[12]Université Libre de Bruxelles, Science Faculty CP230, B-1050 Brussels, Belgium
[13]Vrije Universiteit Brussel, Dienst ELEM, B-1050 Brussels, Belgium
[14]Department of Physics, Chiba University, Chiba 263-8522, Japan
[15]Department of Physics and Astronomy, University of Canterbury, Private Bag 4800, Christchurch, New Zealand
[16]Department of Physics, University of Maryland, College Park, Maryland 20742, USA
[17]Department of Physics and Center for Cosmology and Astro-Particle Physics, Ohio State University, Columbus, Ohio 43210,
[18]Department of Astronomy, Ohio State University, Columbus, Ohio 43210, USA
[19]Department of Physics, TU Dortmund University, D-44221 Dortmund, Germany
[20]Department of Physics, University of Alberta, Edmonton, Alberta T6G 2E1, Canada
[21]Département de physique nucléaire et corpusculaire, Université de Genève, CH-1211 Genève, Switzerland
[22]Department of Physics and Astronomy, University of Gent, B-9000 Gent, Belgium
[23]Department of Physics and Astronomy, University of California, Irvine, California 92697, USA
[24]Laboratory for High Energy Physics, École Polytechnique Fédérale, CH-1015 Lausanne, Switzerland
[25]Department of Physics and Astronomy, University of Kansas, Lawrence, Kansas 66045, USA
[26]Department of Astronomy, University of Wisconsin, Madison, Wisconsin 53706, USA
[27]Department of Physics and Wisconsin IceCube Particle Astrophysics Center, University of Wisconsin, Madison, Wisconsin 53706, USA
[28]Institute of Physics, University of Mainz, Staudinger Weg 7, D-55099 Mainz, Germany
[29]Université de Mons, 7000 Mons, Belgium
[30]TU Munich, D-85748 Garching, Germany
[31]Bartol Research Institute and Department of Physics and Astronomy, University of Delaware, Newark, Delaware 19716, USA
[32]Department of Physics, University of Oxford, 1 Keble Road, Oxford OX1 3NP, United Kingdom
[33]Department of Physics, University of Wisconsin, River Falls, Wisconsin 54022, USA
[34]Oskar Klein Centre and Department of Physics, Stockholm University, SE-10691 Stockholm, Sweden
[35]Department of Physics and Astronomy, Stony Brook University, Stony Brook, New York 11794-3800, USA
[36]Department of Physics, Sungkyunkwan University, Suwon 440-746, Korea
[37]Department of Physics and Astronomy, University of Alabama, Tuscaloosa, Alabama 35487, USA
[38]Department of Astronomy and Astrophysics, Pennsylvania State University, University Park, Pennsylvania 16802, USA
[39]Department of Physics, Pennsylvania State University, University Park, Pennsylvania 16802, USA
[40]Department of Physics and Astronomy, Uppsala University, Box 516, S-75120 Uppsala, Sweden
[41]Department of Physics, University of Wuppertal, D-42119 Wuppertal, Germany
[42]DESY, D-15735 Zeuthen, Germany
[43]Max-Planck-Institut für Physik, D-80805 München, Germany

(Received 16 May 2013; published 19 August 2013)

We present the first statistically significant detection of neutrino oscillations in the high-energy regime (>20 GeV) from an analysis of IceCube Neutrino Observatory data collected in 2010 and 2011. This measurement is made possible by the low-energy threshold of the DeepCore detector (~ 20 GeV) and benefits from the use of the IceCube detector as a veto against cosmic-ray-induced muon background. The oscillation signal was detected within a low-energy muon neutrino sample (20–100 GeV) extracted from data collected by DeepCore. A high-energy muon neutrino sample (100 GeV–10 TeV) was extracted from IceCube data to constrain systematic uncertainties. The disappearance of low-energy upward-going muon neutrinos was observed, and the nonoscillation hypothesis is rejected with more than 5σ significance. In a two-neutrino flavor formalism, our data are best described by the atmospheric neutrino oscillation parameters $|\Delta m^2_{32}| = (2.3^{+0.6}_{-0.5}) \times 10^{-3}$ eV^2 and $\sin^2(2\theta_{23}) > 0.93$, and maximum mixing is favored.

DOI: 10.1103/PhysRevLett.111.081801 PACS numbers: 14.60.Pq, 14.60.Lm, 95.55.Vj, 95.85.Ry

Neutrino flavor oscillations are now an established fact. A number of experiments have observed this physical phenomenon over a wide range of energies, spanning from a fraction of MeV to several GeV. Measurements above 10 GeV have been relatively limited because of constraints of detector volume, neutrino beam energy, and/or insufficient distance of the detector to the beam source. With the construction of high-energy neutrino telescopes with very large volumes and abundant atmospheric neutrinos, studies of neutrino properties above 10 GeV have become possible. Recently, the ANTARES Collaboration reported a first indication (2.3σ) of atmospheric neutrino oscillations in the 20 to 100 GeV energy band [1]. In this Letter, we report the first statistically significant observation of atmospheric ν_μ disappearance in this energy band.

Flavor oscillations of atmospheric neutrinos traversing Earth are a complex process, since all three active flavors may transform into one another. Furthermore, matter effects modify the effective oscillation parameters in Earth from the vacuum values. However, for the energy range of this analysis, a two-flavor vacuumlike description ($\nu_\mu \to \nu_\tau$) is

an adequate approximation. In this scenario, the muon neutrino survival probability is

$$P(\nu_\mu \rightarrow \nu_\mu) = 1 - \sin^2(2\theta_{23})\sin^2(1.27\Delta m^2_{32} L/E), \quad (1)$$

where Δm^2_{32} is the atmospheric mass-squared difference in eV^2, θ_{23} is the atmospheric mixing angle, L is the propagation distance in kilometers, and E is the neutrino energy in GeV. Full numerical three-flavor calculations in matter found differences from this formula of less than a few percent. Given the resolution of the present analysis, this approximation is sufficiently accurate.

This analysis uses data collected from May 2010 to May 2011 by the IceCube neutrino telescope, including its low-energy subdetector DeepCore [2]. IceCube is a cubic-kilometer neutrino detector installed in the ice at the geographic South Pole [3]. Neutrino detection relies on the optical detection of Cherenkov radiation emitted by secondary particles produced in neutrino interactions in the surrounding ice or the nearby bedrock. This analysis detects muons produced in charged current interactions of ν_μ which can travel large distances in the ice. Their long tracks can be reconstructed and provide information about the direction of the initial neutrino. IceCube's optical sensors, digital optical modules (DOMs), consist of 25.4 cm photomultiplier tubes in a glass pressure housing with *in situ* pulse digitization [4,5]. The sensors are arranged on 86 vertical strings, each holding 60 DOMs. The primary (high-energy) detector has a spacing of 17 m between sensors and an average horizontal distance of 125 m between neighboring strings. The low-energy infill array DeepCore consists of eight dedicated strings with a typical spacing of 70 m deployed near the center of the IceCube array. On the dedicated DeepCore strings, the sensors are concentrated in the clearest deep ice, with a denser 7 m vertical spacing. This analysis uses data taken while 79 detector strings were operational (IceCube-79), including six of the dedicated DeepCore strings. A total of 318.9 days of high-quality data was collected in this configuration, excluding periods of calibration runs, partial detector configurations, and detector downtime.

The aim of this analysis was to experimentally measure an expected modification of the atmospheric neutrino zenith angle distribution due to oscillation-induced muon neutrino disappearance. From Eq. (1), we expected the effect to be strongest for vertical events with neutrino energies around 25 GeV. Two samples of upward-going muon neutrino events [$\cos(\text{zenith angle}) < 0$] were extracted from data. The first sample was obtained from relatively high-energy events using data from the entire IceCube detector. The second sample, selected from events starting in the DeepCore volume, was very pure in lower-energy neutrinos after using the surrounding IceCube array as an active veto to reject atmospheric muon background and high-energy (> 100 GeV) neutrinos [6]. Standard neutrino oscillations are expected to affect only the low-energy sample. The high-energy reference sample provided high statistics outside the signal region and served to constrain systematic uncertainties. The low-energy sample contained 719 events, while the high-energy sample contained 39 638 events after final cuts.

The directions of the neutrino-induced muon tracks in the high-energy sample were determined with the standard maximum likelihood muon track reconstruction of IceCube [7]. For low-energy events, the same method was applied as an initial step. However, the standard hypothesis of a through-going track is not appropriate at low energies. In a subsequent step, the length and end points of the track are reconstructed and the likelihood of whether the track started and/or stopped inside the detector volume is calculated [6]. Misreconstructed downward-going tracks originating from cosmic-ray muons are rejected by quality cuts on reconstruction variables like the number of unscattered photons and the track likelihood. The resultant neutrino energy distributions of the two samples are shown in Fig. 1.

The dominant background in the low-energy sample was misidentified (as tracklike) ν_e events, with a contribution of 10%–15% as estimated from simulations. The event selection has a nonzero efficiency for ν_τ events, and some of the ν_μ that oscillate into ν_τ will thus be retained in the sample. We therefore included the ν_e background and the effect of ν_τ appearance due to $\nu_\mu \rightarrow \nu_\tau$ in the analysis. In 11 days of simulated cosmic-ray air shower data, no events were found to pass the final cuts of the low-energy sample. The dominant background in the high-energy sample was misreconstructed cosmic-ray-induced muons contributing 5%.

The resolution of the reconstructed zenith angle is an essential parameter, given that the neutrino propagation length is proportional to the cosine of the zenith angle. The variation in zenith angles alters L/E and thus the survival probability. The angular resolution of the low-energy sample was 8° with respect to the neutrino direction, roughly independent of direction and only slightly

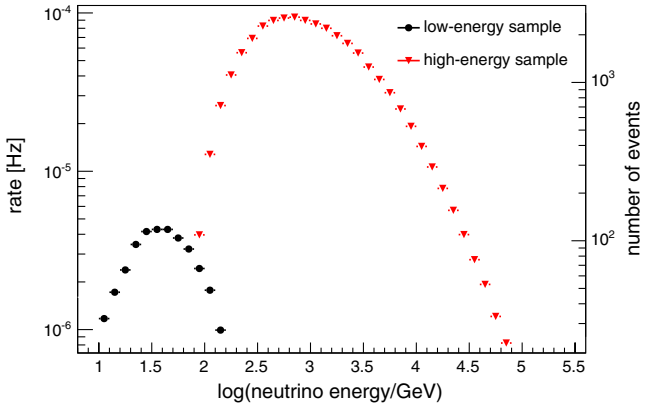

FIG. 1 (color online). Expected distribution of the neutrino energy of atmospheric neutrinos in the low-energy (DeepCore) and high-energy (IceCube) samples according to simulations.

degrading with decreasing energy. The angle between the neutrino and the muon produced in a charged current interaction amounts to about half of the measured zenith resolution.

We tested for an oscillation signal by evaluating the combined χ^2 for histograms of the cosine of the reconstructed zenith angle for both the high-energy and the low-energy samples. A bin size of 0.1 resulted in 20 bins. Systematic uncertainties, considered via the covariance matrix σ_{ij}, give $\chi^2 = \sum_{ij} R_i R_j \sigma_{ij}^{-2}$. Here, R_i is the difference between the expected and measured rates in bin number i. The covariance matrix is defined as $\sigma_{ij}^2 = \delta_{ij} u_i u_j + \sum_k c_i^k c_j^k$ and depends on uncorrelated (statistical) errors (u_i) in each bin as well as on correlated (systematic) errors ($c_i^k = n_i^{\mathrm{std}} - n_i^{\mathrm{syst},k}$). This approach implies the linear additive superposition of systematic errors. The term $n_i^{\mathrm{syst},k}$ is the expected event rate in bin i after modification of the kth systematic source of error by 1σ, and n_i^{std} is the default expectation in the same bin [8]. Hence, the off-diagonal elements of the covariance matrix reflect the bin-to-bin correlations of the systematic uncertainties, as expected. A set of sources of systematic uncertainties was considered explicitly and propagated by Monte Carlo simulation to the final selection level. Included are the absolute sensitivity of the IceCube sensors ($\pm 10\%$) and the efficiency of the more sensitive DeepCore DOMs relative to the standard IceCube DOMs (1.35 ± 0.03), the optical parameters (scattering and absorption) of the ice as a detector medium where the uncertainty is estimated by the difference of the optical parameters obtained by the extraction methods [9,10]. An additional systematic uncertainty for this analysis is associated with the atmospheric neutrino flux expectation given by Ref. [11]. Recent measurements of the spectrum of charged cosmic rays in the energy range 200 GeV to 100 TeV (e.g., Ref. [12]) indicate a flatter cosmic-ray spectrum than that assumed in Ref. [11]. To reflect these new measurements, we adjusted the neutrino spectrum by hardening the spectral index by 0.05. Around this expectation, we considered uncertainties in the absolute normalization ($\pm 25\%$), the spectral index (± 0.05), as well as the difference between the calculations by Refs. [11,13] for ν_μ and for ν_e.

The χ^2 was evaluated for two different physics hypotheses: a standard oscillation scenario with the world average best-fit parameters [14] and the nonoscillation scenario. The predicted zenith angle distributions for both hypotheses are shown in Fig. 2 together with the data. We note good agreement between predictions and data in both low- and high-energy (reference) samples. With $\Delta\chi^2 = 30$ between these hypotheses, a nonoscillation scenario is

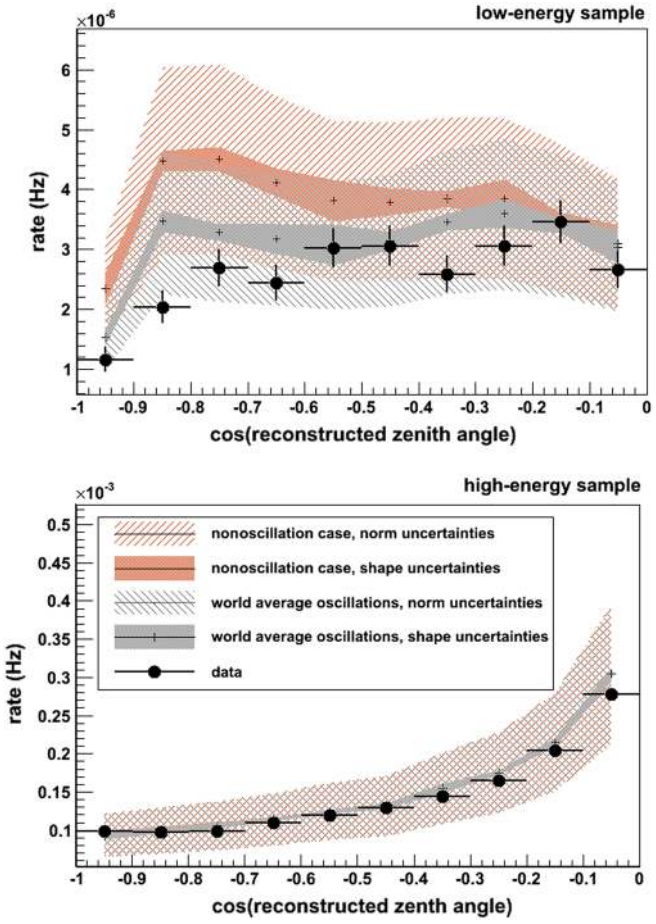

FIG. 2 (color online). Data and Monte Carlo expectation at world average oscillation parameters [$\sin^2(\theta_{23}) = 0.995$ and $|\Delta m_{32}^2| = 2.39 \times 10^{-3}$ eV^2] [14] and at the nonoscillation scenario for the low-energy and high-energy samples. For the purpose of illustration, systematic uncertainties are split into a fully correlated (norm) part and an uncorrelated (shape) part. Both components are indicated by shaded error bands. The χ^2 fit is performed jointly on both samples to better control systematics; in particular, the normalizations of the two samples are substantially correlated, so that accommodating the low-energy data under the nonoscillation hypothesis would lead to inconsistency with the high-energy sample.

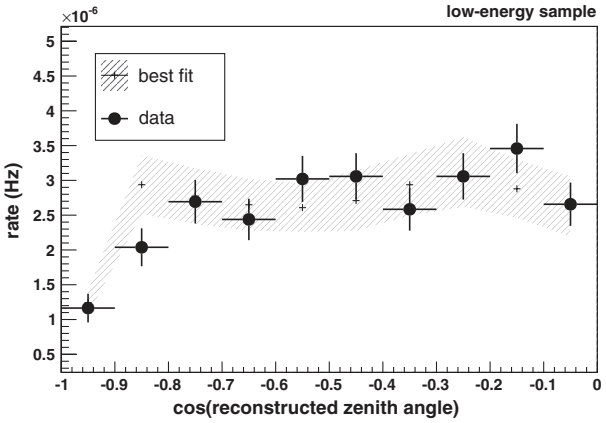

FIG. 3. Data and Monte Carlo expectation at best-fit oscillation parameters and pulls for the low-energy sample. The systematic uncertainty band is derived from the fit uncertainties of the pulls.

TABLE I. Pulls on the systematic uncertainties at the best-fit value of $|\Delta m^2_{32}| = 2.3 \times 10^{-3}$ eV^2 and $\sin^2(2\theta_{23}) = 1$.

Systematic uncertainty	Pull (standard deviations)
DOM efficiency	0.32
Ice model	−0.12
Atmospheric flux model	−0.59
Normalization	−0.82
Cosmic ray index or cross section	0.42
Relative efficiency of DeepCore DOMs	−0.01
Normalization of ν_e	−0.53

rejected with a p value of 10^{-8} or 5.6σ. The significance was evaluated with a toy Monte Carlo simulation to account for deviations from a χ^2 distribution, since neither assumed hypothesis necessarily corresponds to the χ^2 minimum.

The χ^2 was also evaluated as a function of the oscillation parameters, using the *pull* method outlined in Ref. [8]. The parameters considered as sources of systematic uncertainty in the Monte Carlo prediction were fitted simultaneously with the oscillation parameters. The expected zenith angle distribution at best fit (oscillation parameters and systematic uncertainties) is shown in Fig. 3 for the low-energy sample. The best-fit systematics parameters (represented by the pulls) are listed in Table I. All pulls were within the 1σ band, indicating a self-consistency of the analysis. The best-fit oscillation parameters are given by $|\Delta m^2_{32}| = 2.3 \times 10^{-3}$ eV^2 and $\sin^2(2\theta_{23}) = 1$, with $\chi^2 = 15.7$ and 18 degrees of freedom (20 bins, 2 fitted parameters).

The two-dimensional confidence regions of the oscillation parameters were determined from the $\Delta\chi^2$ around the best fit with 2 degrees of freedom. The resultant regions are shown in Fig. 4 together with results from other experiments [15,16]. A full Monte Carlo ensemble test, sampling true values for the considered sources of systematic errors according to Gaussian statistics and Poisson fluctuations in the observed bin counts, was used to map the test statistics. A slight overcoverage at 78% was found for the 1σ contour, related to the proximity of the mixing angle to the maximum mixing boundary; i.e., the obtained contours are conservative. The confidence regions for the individual parameters were determined by marginalization analogous to a profile likelihood method. We obtain 68% confidence intervals of $|\Delta m^2_{32}| = (2.3^{+0.5}_{-0.6}) \times 10^{-3}$ eV^2 and $\sin^2(2\theta_{23}) > 0.93$ using a $\Delta\chi^2$ with 1 degree of freedom.

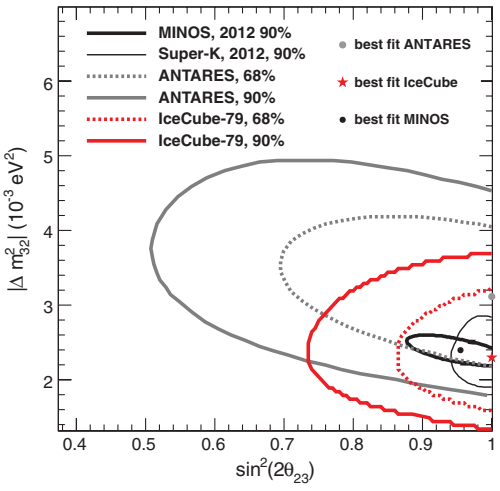

FIG. 4 (color). Significance contours for the presented atmospheric neutrino oscillation analysis, compared with the results of ANTARES [1], MINOS [15], and SuperKamiokande [16].

This analysis of IceCube data has provided the first significant detection ($>5\sigma$) of atmospheric neutrino oscillations at energies near the 25 GeV oscillation maximum for vertical events. The measured oscillation parameters are in good agreement with results from other experiments that have measured the atmospheric oscillation parameters with high resolution at lower energies. Hence, these measurements agree with the theoretical predictions of the standard three-neutrino flavor oscillation framework. Significant future improvements in our sensitivity to atmospheric neutrino oscillations are expected by the application of new reconstruction methods that are more efficient at the lowest energies covered by DeepCore. We expect that the rate of detected atmospheric neutrinos near the 25 GeV oscillation maximum will be increased significantly. These higher statistics will lead to tighter constraints on the oscillation parameters with IceCube. Furthermore, the inclusion of the reconstructed energy as a second analysis variable will improve the constraints in particular on Δm^2_{32}. Additionally, improvement is expected from the inclusion of the two final DeepCore strings which started taking data in May 2011.

We acknowledge support from the following agencies: U.S. National Science Foundation—Office of Polar Programs, U.S. National Science Foundation—Physics Division, University of Wisconsin Alumni Research Foundation, the Grid Laboratory of Wisconsin (GLOW) grid infrastructure at the University of Wisconsin-Madison, the Open Science Grid (OSG) infrastructure, U.S. Department of Energy and National Energy Research Scientific Computing Center, the Louisiana Optical Network Initiative (LONI) grid computing resources, USA; Natural Sciences and Engineering Research Council of Canada, WestGrid, and Compute/Calcul, Canada; Swedish Research Council, Swedish Polar Research Secretariat, Swedish National Infrastructure for Computing (SNIC), and Knut and Alice Wallenberg Foundation, Sweden; German Ministry for Education and Research (BMBF), Deutsche Forschungsgemeinschaft (DFG), Helmholtz Alliance for Astroparticle Physics (HAP), Research Department of Plasmas with Complex Interactions (Bochum), Germany; Fund for Scientific Research (FNRS-FWO), FWO Odysseus programme,

Flanders Institute to encourage scientific and technological research in industry (IWT), Belgian Federal Science Policy Office (Belspo), Belgium; University of Oxford, United Kingdom; Marsden Fund, New Zealand; Australian Research Council; Japan Society for Promotion of Science (JSPS), Japan; and the Swiss National Science Foundation (SNSF), Switzerland.

*Present address: Physics Department, South Dakota School of Mines and Technology, Rapid City, SD 57701, USA.
†Corresponding author.
Andreas.Gross@tum.de
‡Present address: Los Alamos National Laboratory, Los Alamos, NM 87545, USA.
§Also at Sezione INFN, Dipartimento di Fisica, I-70126, Bari, Italy.
‖Present address: NASA Goddard Space Flight Center, Greenbelt, MD 20771, USA.

[1] S. Adrian-Martinez *et al.* (ANTARES Collaboration), Phys. Lett. B **714**, 224 (2012).
[2] R. Abbasi *et al.* (IceCube Collaboration), Astropart. Phys. **35**, 615 (2012).
[3] A. Achterberg *et al.* (IceCube Collaboration), Astropart. Phys. **26**, 155 (2006).
[4] R. Abbasi *et al.* (IceCube Collaboration), Nucl. Instrum. Methods Phys. Res., Sect. A **601**, 294 (2009).
[5] R. Abbasi *et al.* (IceCube Collaboration), Nucl. Instrum. Methods Phys. Res., Sect. A **618**, 139 (2010).
[6] O. Schulz *et al.* (IceCube Collaboration), Proceedings of the 31st ICRC, Lodz, Poland, 2009, http://icrc2009.uni.lodz.pl/proc/html/index.php_id=17.html.
[7] J. Ahrens *et al.* (AMANDA Collaboration), Nucl. Instrum. Methods Phys. Res., Sect. A **524**, 169 (2004).
[8] G. L. Fogli, E. Lisi, A. Marrone, D. Montanino, and A. Palazzo, Phys. Rev. D **66**, 053010 (2002).
[9] M. Ackermann *et al.* (AMANDA Collaboration), J. Geophys. Res. **111**, D13203 (2006).
[10] M. Aartsen *et al.* (IceCube Collaboration), Nucl. Instrum. Methods Phys. Res., Sect. A **711**, 73 (2013).
[11] M. Honda, T. Kajita, K. Kasahara, S. Midorikawa, and T. Sanuki, Phys. Rev. D **75**, 043006 (2007).
[12] Y. Yoon *et al.*, Astrophys. J. **728**, 122 (2011).
[13] G. D. Barr, T. K. Gaisser, P. Lipari, S. Robbins, and T. Stanev, Phys. Rev. D **70**, 023006 (2004).
[14] G. Fogli, E. Lisi, A. Marrone, A. Melchiorri, A. Palazzo, A. Rotunno, P. Serra, J. Silk, and A. Slosar, Phys. Rev. D **78**, 033010 (2008).
[15] R. Nichol *et al.* (MINOS Collaboration), Nucl. Phys. B, Proc. Suppl. **235-236**, 105 (2013).
[16] Y. Itow, Nucl. Phys. B, Proc. Suppl. **235-236**, 79 (2013).